UPPSALA
UNIVERSITET

Digital Comprehensive Summaries of Uppsala Dissertations from the Faculty of Science and Technology 1233

High-Temperature Microfluidics for Space Propulsion

VILLE LEKHOLM

ACTA
UNIVERSITATIS
UPSALIENSIS
UPPSALA
2015

ISSN 1651-6214
ISBN 978-91-554-9186-4
urn:nbn:se:uu:diva-246057

Dissertation presented at Uppsala University to be publicly examined in 2001, Ångströmlaboratoriet, Lägerhyddsvägen 1, Uppsala, Friday, 24 April 2015 at 09:15 for the degree of Doctor of Philosophy. The examination will be conducted in English. Faculty examiner: Professor Herbert Shea (École polytechnique fédèrale de Lausanne).

Abstract
Lekholm, V. 2015. High-Temperature Microfluidics for Space Propulsion. *Digital Comprehensive Summaries of Uppsala Dissertations from the Faculty of Science and Technology* 1233. 50 pp. Uppsala: Acta Universitatis Upsaliensis. ISBN 978-91-554-9186-4.

In this thesis, microfabrication methods and tools for analysis of heated cold-gas microthrusters are presented, with the aim of improving their reliability and performance. Cold-gas thrusters operate by accelerating pressurized gas through a nozzle. These thruster systems are very straightforward in both design and operation, relying on little more than a pressurized tank, a valve, and a nozzle. This makes them suitable for miniaturization, enabling their use on very small spacecraft. However, an inherent drawback with cold-gas thrusters is their low propellant efficiency – in thrusters known as specific impulse, or I_{sp}. This is compounded by the fact that when reducing length, the volume, e.g., that of the propellant tank, reduces with the cube of the length, meaning that the maximum amount of storable fuel reduces quickly. Hence, maximizing fuel efficiency is even more important in miniaturized systems. Still, because of their other advantages, they remain suitable for many missions. Schlieren imaging – a method of visualizing differences in refractive index – was used thrughout this thesis to visualize exhaust jets from microthrusters, and to find leaks in the components. It was found that effects of the processing of conventionally fabricated silicon nozzles, resulted in a misalignment of up to 3° from the intended thrust vector, increasing propellant consumption by up to 5%, and potentially causing unintended off-axis acceleration of the spacecraft. Schlieren imaging was also used to verify that the exhaust from thrusters fabricated with close to circular cross-sections was well behaved. These nozzles did not suffer from the previous misalignment issue, and the shape of the cross-section decreased viscous losses. For applications requiring higher temperatures, a microthruster nozzle with an integrated flow sensor was fabricated from tape cast yttria stabilized zirconia. The ceramic substrate enabled heater temperatures of the nozzle exceeding 1000 °C, resulting in an increase in I_{sp} of 7.5%. Integration of a flow sensor allowed the elimination of couplings and reduced the number of interfaces, thereby reducing the overall risk of failure. Close integration of the sensor allowed moving the point of measurement closer to the nozzle, enabling improved reliability of the measurements of the propellant consumption. The temperature of the heater, in combination with the ion conductive properties of the substrate proved to be a limiting factor in this design. Two routes were explored to overcome these problems. One was to use the temperature dependence of the ion conductivity as a sensing principle, thereby demonstrating a completely new flow sensor principle, which results in better calibration, tighter integration, and 9 orders of magnitude stronger signal. The other was using hafnium oxide, or hafnia, as a structural material for high-temperature micro-electromechanical systems. This involved developing a recipe for casting hafnia ceramic powder, and determining the Young's modulus and thermal shock resistance of the cast samples, as well as studying the minimum feature size and maximum aspect ratio of cast microstructures.

Ville Lekholm, Department of Engineering Sciences, Microsystems Technology, 516, Uppsala University, SE-751 20 Uppsala, Sweden.

ISSN 1651-6214
ISBN 978-91-554-9186-4
urn:nbn:se:uu:diva-246057 (http://urn.kb.se/resolve?urn=urn:nbn:se:uu:diva-246057)

To Edvard and Emilia, with love

List of papers

This thesis is based on the following papers, which are referred to in the text by their Roman numerals.

I **Ville Lekholm**, Kristoffer Palmer, Greger Thornell (2012) Schlieren imaging of microthruster exhausts for qualitative and quantitative analysis. *Measurement Science and Technology* 23 (8), 085403

II Kristoffer Palmer, Ernesto Vargas Catalan, **Ville Lekholm**, Greger Thornell (2013) Investigation of exhausts from fabricated silicon micronozzles with rectangular and close to rotationally symmetric cross-sections. *Journal of Micromechanics and Microengineering* 23 (10), 105001

III **Ville Lekholm**, Anders Persson, Kristoffer Palmer, Fredric Ericson, and Greger Thornell (2013) High-temperature zirconia microthruster with an integrated flow sensor. *Journal of Micromechanics and Microengineering* 23 (5), 055004

IV **Ville Lekholm**, Anders Persson, Lena Klintberg and Greger Thornell (2015) Investigation of a zirconia co-fired ceramic calorimetric microsensor for high-temperature flow measurements. Accepted for publication in *Journal of Micromechanics and Microengineering*

V Anders Persson, **Ville Lekholm**, Greger Thornell and Lena Klintberg (2015) A high-temperature calorimetric flow sensor employing ion conduction in zirconia. Submitted to *Applied Physics Letters*

VI **Ville Lekholm**, Anders Persson, Lena Klintberg, Greger Thornell (2015) Hafnium oxide for high-temperature micorelectromechanical systems. Submitted to *Journal of Micromechanics and Microengineering*

Author’s contribution

Paper I	Major part of planning, most of experiments, analysis and writing.
Paper II	Major part of experiments, analysis and writing.
Paper III	Most of planning, experiments, analysis and writing.
Paper IV	Major part of planning, most of experiments, analysis and writing.
Paper V	Major part of planning experiments and analysis, part of writing.
Paper VI	Most of planning, experiments, analysis and writing.

Contents

List of Abbreviations

Δv	Velocity change
μ	micro, 1×10^{-6}
CT	Computed tomography
DRIE	Deep reactive ion etching
FEEP	Field emission electric propulsion
GPS	Global positioning system
HTCC	High-temperature co-fired ceramics
I_{sp}	Specific impulse
IC	Integrated circuit
LEO	Low earth orbit
LTCC	Low-temperature co-fired ceramics
MEMS	Microelectromechanical systems
MST	Microsystems technology
PCB	Printed circuit-board
PDMS	Polydimethylsiloxane, a silicon rubber
PPT	Pulsed Plasma Thrusters
RF	Radio frequency
RIE	Reactive ion etching
SOFC	Solid-oxide fuel cells
YSZ	Yttria-stabilized zirconia
YSZ8	8 mol-% yttria-stabilized zirconia

1. Introduction

> “What are the possibilities of small but movable machines? They may or may not be useful, but they surely would be fun to make.”
>
> — Richard P. Feynman

On February 14, 1990, the spacecraft Voyager 1, its primary mission long since completed, turned its camera toward the Earth and captured one of the most famous images of our planet known as the "Pale Blue Dot," Figure 1.1. Transmitted to earth at the speed of light, it took nearly five and a half hours to reach us. To see our home, fainter than a star in the night sky, truly puts our existence on earth into perspective. It is also an example of our, rightfully, insatiable fascination with our own planet. As our understanding of physics, biology, and chemistry increases, so does the desire to learn even more.

To say that space technology has matured in its role in our everyday life, would be an understatement. We take reliable weather forecasts, high resolution images of our regional terrain, and lag-free long distance phone calls for granted. Today, it is difficult to find a cellular phone that do not include a GPS receiver, and this technology is even being included in both compact cameras and watches. A car without satellite navigation is either old, or entry-level from a low end brand. Yet, while these technologies are used by millions of people every day without a second thought, they all rely on satellites capturing and relaying data and, arguably, represent some of the greatest scientific achievements in recent decades. It is probably not undeserved that "rocket science", in daily speech, has come to represent the pinnacle of research. Yet, while acknowledging how awesome these achievements are, in the literal sense of the word, they are also taken for granted as the baseline of technology, "We can land a man on the moon, but I can’t get hot coffee?" Even space tourism has become a buzz-topic recently, suggesting that we are either ignoring, forgetting, or, most likely, simply not realizing the tremendous effort associated with the development, manufacture, and rigorous testing of spacecraft. Launching spacecraft is still very much a challenge and remains high risk, high cost, and requires long preparation.

Despite these factors, there are constantly new missions conceived to improve our understanding of our planet, space, and our improbable origin. In the words of one of the fathers of rocket science, Dr. Wernher

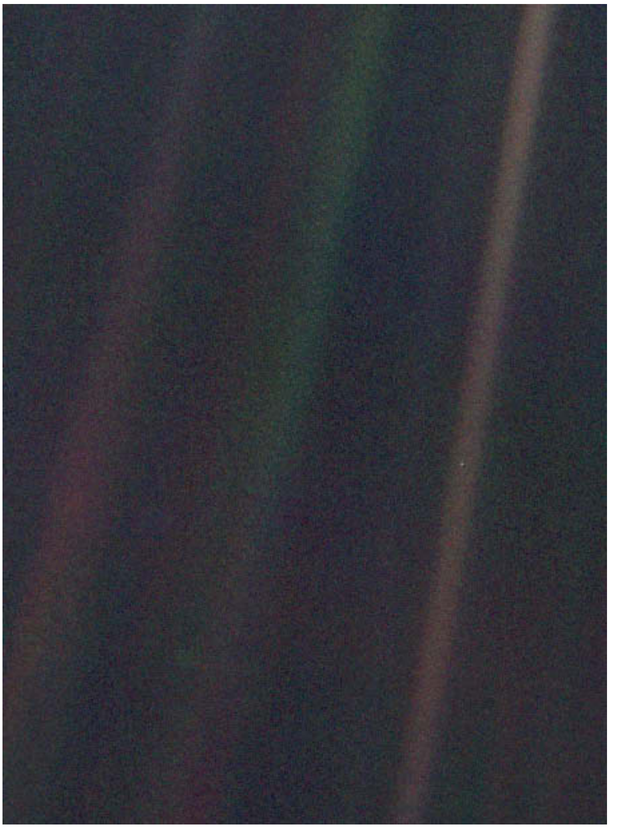

Figure 1.1. Pale Blue Dot. A picture of Earth, as seen from about 6 billion kilometers, taken by the space probe Voyager 1. Earth is visible just below the center of the image, in the lighter band to the right. Courtesy NASA/JPL-Caltech.

von Braun, "Man has already poked his nose into space, and he is not likely to pull it back." In order to increase the accessibility to researchers, students, and the general public, it is vital to reduce the size and mass of spacecraft, consequently reducing the launch cost which represents a major part of the total cost of a project. However, the measures to reduce the cost require the use of new technology. Herein lies somewhat of a catch 22. Because of the high cost, the tolerance for failure is very low and leads to the choice of "tried-and-true" over new technology. This, in turn, limits size and weight reductions to what follows from the evolutionary progression in the electronics and machining industry. However, the technology which could reduce the mass of spacecraft by orders of magnitude exists, and the industry is starting to move in this direction.

Microelectromechanical systems (MEMS) technology has sprouted from the electronics industry as a way to fabricate microscale electromechanical or fluidic components. The tools and fabrication techniques used are often developed for semiconductor electronics but are tweaked or used slightly differently to achieve the desired structures. *Micro* (μ) is a prefix indicating 10^{-6}, or 0.000001, and 1 micrometer (μm), the typical length scale in MEMS components, is approximately one hundredth of the thickness of the paper on which this thesis is printed. But besides being very small, there are other factors involved as well, and reducing the size of a component can be easier or harder to achieve, and more or less beneficial.

While some systems occupy a certain volume due to the size of the technology contained within, other systems require a certain size for other, physical reasons. Examples include antennas and optics, both of which collect electromagnetic radiation. Antennas need to be a certain length in order to register a complete wavelength, and suffer from performance reduction when made smaller. Optics collect light, and the size of the lens element, or aperture, determines the strength of the signal, which translates to signal-to-noise ratio in the images. Due to limitations such as these, simple physics restricts how small certain components can be made. Size reductions also lead to changes in the requirements placed on components. As the mass or moment of inertia of a craft decreases, so does the force, or impulse, necessary to cause a change in velocity or rotational speed. In other instances, the reduction in size can be unequivocally favorable. For example, bringing a pot of water to boil can be both frustrating and time consuming, whereas bringing a droplet of water to boil requires very little power and can be achieved almost instantly, even though the specific heat capacity of the material is unchanged.

These examples all relate to a phenomenon known as scaling. When the size decreases, the area decreases as the square of the length. On the other hand, the volume, and hence the mass, decreases as the cube of the length. Depending on the application, this can be either beneficial or detrimental, and in some cases, the reduction in size can lead to a switch in the dominating physical principle. If larger animals walk into water, gravitation dominates and they sink. With insects, the surface tension is the dominating force, and they can sit on the surface of ponds. In fluidics, macroscopic flows are typically dominated by inertial forces which cause turbulence and whirling of the liquid, but in smaller scales the flows are dominated by viscous forces and are parallel, or *laminar*. This is due to the increased influence of the perimeter since the boundary layer thickness remains the same. Hence, the geometry of a small channel plays a larger roll than that of a large one.

When it comes to satellites and other spacecraft, certain components are harder to miniaturize than others. Once launched, they are typically designed to be entirely self-reliant. Every redirection of a camera, solar panel or antenna, can be commanded from ground control, but needs to be achieved by the spacecraft itself. The same goes for any reorientation of the craft (known as attitude control), or orbit adjustment, including those necessary to counter loss of altitude through aerodynamic drag. In order to achieve these maneuvers, some type of propulsion is necessary. Regardless of application, space or otherwise, these are governed by Newton's third law of motion; for every action, there is an equal and opposite reaction. For example, the action of a car's wheels rotating against pavement results in an equal but opposite force from the pavement on the wheels which accelerates the car forward. In space, the force is typically achieved by expelling mass through a nozzle, resulting in a reactive force in the opposite direction. "Propulsion system", then, refers to everything related to the propulsion. In the example with the car, the propulsion system would consist of the fuel tank, engine, gearbox, drive train, and wheels.

In micropropulsion systems, the "micro" can refer to either of two things: either it refers to a propulsion system which delivers thrust in the order of micronewton (μN), such as those used for very precise attitude control of larger spacecraft, e.g., the Hubble Space Telescope, or the LISA [1] or Darwin [2] missions; or the term refers to propulsion systems which are in the μm-scale, not excluding those which also produce μN thrust. The former does not have the same requirements on maximum size or mass, and the latter can be designed to produce more or less thrust. Current micropropulsion includes both chemical and electrical systems. Chemical propulsion relies on chemical reactions to create thrust, such as through combustion or decomposition of a propellant. Cold-gas thrusters, which expel pressurized gas through a nozzle, are generally included in this category. The function of electrical propulsion, on the other hand, relies on the acceleration of charged particles in an electric field.

When it comes to attitude control of small spacecraft, cold gas microthrusters are very straightforward in operating principle, and do not require large peripheral systems. However, cold gas propulsion systems generally have very low efficiency, in rockets and thrusters referred to as specific impulse, I_{sp}, and, all else being equal, lower I_{sp} means more propellant is needed.

The aim of this thesis is to present fabrication techniques for cold gas microthrusters for use in small spacecraft, which improve on previous designs both in efficiency and control. To improve the efficiency of the thrusters, it is essential to make sure they operate as designed, and a technique called schlieren imaging is used in **Papers I**, **II**, and **III** to identify leaks and to visualize the thrust vector to identify misalignments. To reduce viscous losses, a fabrication route is explored in **Paper II** which results in close to circular symmetric thruster nozzles. Another point of improvement is to raise the temperature of the expelled gas. This increases the specific impulse thereby reducing the amount of necessary propellant. In **Paper III**, yttrium oxide stabilized zirconium oxide (known as yttria and zirconia, respectively) high-temperature co-fired ceramic (HTCC) tape is used to fabricate a thruster component capable of surviving temperatures in excess of 1000 °C. Furthermore, to improve control, precise measurement of the propellant flow is vital. The integration of a calorimetric flow sensor with a ceramic thruster is demonstrated in **Paper III**, and a closer examination of the flow sensor is offered in **Paper IV**. In **Paper V**, a new flow sensor principle is proposed, relying on the ion conductivity of zirconia, which allows very close integration with a heated nozzle. Finally, in **Paper VI** the use of hafnium oxide, or hafnia, as a structural material is detailed. Hafnia survives temperatures surpassing the maximum operating temperatures of almost all other ceramics, and does not suffer from ion condictivity to the same extent as yttria stabilized zirconia.

2. Miniaturization

Miniaturization is a broad term describing the trend, particularly in technology, to manufacture things smaller and smaller. This is made possible, for example, by improvements in machining and materials, which reduce the minimum feature size and allow higher precision, thereby enabling smaller devices and reducing the necessary margins, respectively. Typically, this evolution in manufacturing reduces the materials used, thereby reducing costs both directly and indirectly, as, for example, reduced weight reduces shipping costs. It can also be desirable from the point of the end user, such as in the cases of portable phones or implantable pacemakers.

Since the mid-1970's, developments in the semiconductor electronics industry has led to the number of transistors that fit in an integrated circuit doubling approximately every two years [3]. This has resulted in increased capabilities of microcomputers, while at the same time reducing their cost and power consumption, which, in turn, has enabled entirely new product categories, e.g., the mobile computer. As the power consumption decreases, so does the necessary battery size, and eventually it is the interface, e.g., our fingers and vision, that limits the size.

But the trend of miniaturization does not just apply to consumer electronics. For space exploration, this reduction in mass is particularly favorable. This can be demonstrated using Tsiolkovsky's rocket equation [4],

$$\Delta v = v_e \ln \frac{m_0}{m_1}, \tag{2.1}$$

where Δv is the necessary change in speed for a maneuver, v_e is the effective exhaust velocity of the rocket used, m_0 is the initial mass of the rocket including propellant, and m_1 is the mass after the propellant is spent, i.e., when only the rocket structure and payload remains. While this is a simplification, ignoring, e.g., atmospheric drag, it it still applicable for calculating rough estimates. Rewriting the equation to calculate the mass fraction of propellant, M_f, that is, the ratio of propellant $(m_0 - m_1)$ to structure and payload, results in

$$M_f = \frac{m_0 - m_1}{m_0} = 1 - e^{-\frac{\Delta v}{v_e}}. \tag{2.2}$$

Since Δv is dictated by the maneuver, and v_e is given by the rocket used, assuming the same desired outcome and the same rocket, it is seen that the mass fraction, M_f, is constant.

For example, to reach Low Earth Orbit (LEO), a Δv of 9300 m/s is necessary [5]. Furthermore, the core stage of Ariane 5, a commonly used launch vehicle, has an exhaust velocity of approximately 4200 m/s [6]. Using these figures in equation 2.2, yields a propellant mass fraction of 89%. The remaining 11% are the structure of the rocket, typically around 10%, and the remaining 1% is the payload. This gives a launcher to payload ratio of 99 to 1. The result is that a small reduction in mass of the payload, will potentially result in a roughly hundred-fold reduction of the total mass. Eventually, with sufficient reductions in mass, completely new and even more efficient launch methods are possible, using carrier planes or fighter jets for the first stage [7–9]. This makes microelectromechanical systems, and the weight savings that come with them, very attractive for space [10–13].

2.1 Silicon MEMS

MEMS is a collective term including sensors and actuators in the micrometer scale. Sensors are components which provide a signal based on a quantity to be measured, for example pressure or oxygen content. Actuators are active components, influencing their surroundings, for example valves and motors. This is a field of research that has grown immensely, in the wake of the semiconductor integrated circuit (IC) industry.

Integrated circuits are several semiconductor electronic components, fabricated together on a single substrate. This integration eliminates interfacing with macro parts between each component, saving considerable material and volume. IC-chips are made by selectively adding and removing material from, most commonly, silicon wafers, by masking parts not to be affected by a process and then removing the mask. This is done to create conductor paths, dielectric layers, diodes and transistors on the top surface, using the wafer as a substrate. The same methods of fabrication have been used to create miniature electromechanical devices [14, 15], utilizing other than the electrical properties of the material. For example, the same process that is used to pattern conductor paths between electrical components can be used to pattern resistive heaters. Similarly, the same process that removes bulk material between components can be used to fabricate channels, filters, vias, and nozzles. Because of the sizes involved, the processes are typically chemical rather than mechanical, often relying on plasma to either deposit (add) or etch (remove) material.

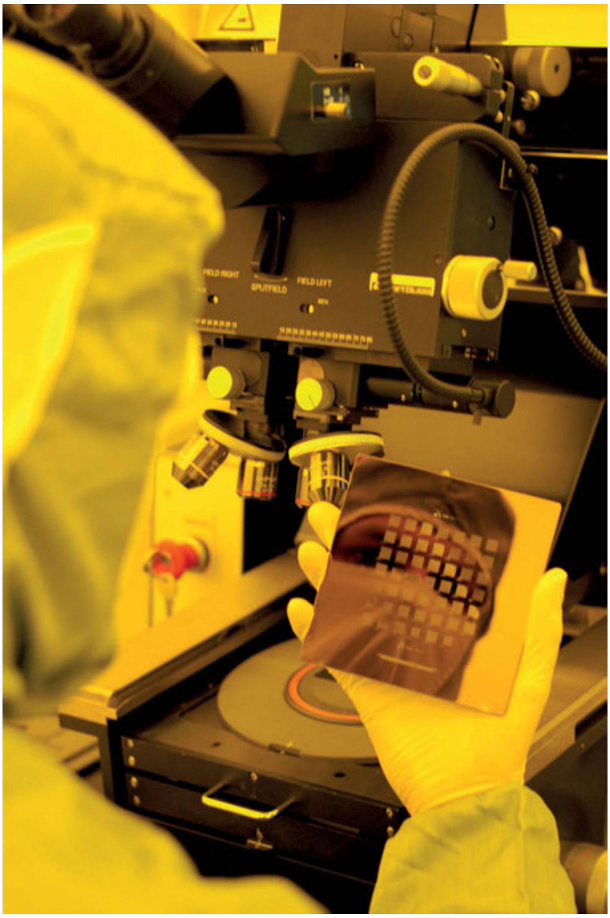

Figure 2.1. A researcher in cleanroom garments inspecting a mask before lithography. The yellow lighting is used to protect materials sensitive to ultraviolet light.

Due to the length scale involved in MEMS manufacturing, extreme levels of cleanliness are required. This is because even a strand of hair or a speck of dust can be the same size or larger than the devices, and may seriously affect the manufacturing process. For this reason, specialized labs, so-called cleanrooms, are used, requiring operators to wear full-body covering clothing, including hood with face mask and hair net, Figure 2.1.

Removing material with reactive ion etching (RIE) is often an isotropic process, meaning the etch rate is independent of direction, Figure 2.2. With RIE, the cavities grow outward at the same rate as downward, and material under the mask is removed. This effect is known as etch undercut, or underetching. However, by alternatively depositing a pacifying layer and etching with an electrical bias on the substrate, it is possible

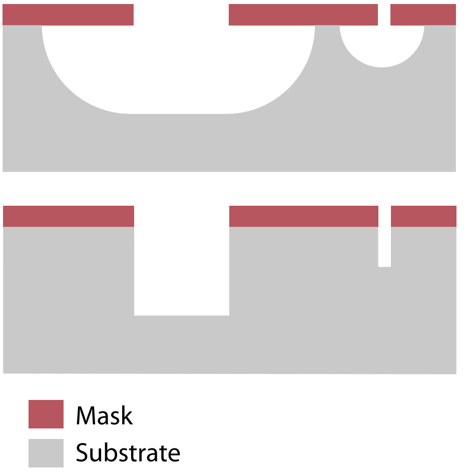

Figure 2.2. Schematic of trenches fabricated using isotropic etching, RIE (top) and anisotropic (directional) etching, DRIE (bottom). The shallower trenches on the right illustrate the effect of RIE lag.

to etch trenches with nearly smooth, vertical side-walls. The latter is a very common process in MEMS fabrication, known as deep reactive ion etching (DRIE).

DRIE is popular because it is easy to control the contours of the patterns. It is therefore ideal for fabrication of channels and cavities, and is often used to fabricate cold gas microthrusters, such as those studied in **Paper I**, benefiting from the smooth side walls [16, 17]. In both RIE and DRIE, the etch depth is typically calculated by etch time. If two different depths are desired in different parts of the wafer, then two different masks are needed. However, there are other ways, like grey-scale lithography or stereolithography [14], to produce different depths in a single mask step, but these require specialized equipment or additional fabrication steps.

In **Paper II**, a fabrication scheme relying on isotropic plasma etching (RIE) and an etch mask consisting of an array of many small openings [18, 19] is proposed. Due to the isotropic nature of the etching, openings sufficiently close to each other will eventually merge and result in a single trench from under-etching. Furthermore, the etch rate is affected by the size of the opening in the mask, Figure 2.2, where a small opening results in a slower etch rate due to a depletion of etching ions – an effect that is known as RIE-lag [20]. With very large openings, on the other hand, a large area of the substrate is exposed and saturates the reactive gas which also leads to a reduction in etch rate. This is known as microloading [21]. Deliberately designing the mask to take advantage of these different effects, the final depth profile of the patterns can be far more elaborate than is otherwise possible with a single mask. In **Paper II**, the mask has been designed to produce half of a micronozzle with a close to circular cross section, i.e., a conical throat and a cylindrical stagnation chamber. Two halves are then bonded to form a full nozzle.

The aforementioned methods describe fabrication using silicon substrates. Silicon is one of the most common materials in MEMS manufacturing and is a natural starting point for many applications. However, there are times when other materials are preferable, particularly if the component is to be used at high temperatures since silicon begins to soften at a few hundred degrees Celsius [22]. In those cases, ceramic materials, which generally have a very high melting point, are preferable [23]. Ceramics can also used in otherwise harsh environments such as in reactive atmospheres [24, 25], which makes them suitable choices for chemical microthrusters.

2.2 Ceramic MEMS

Ceramic materials such as aluminum oxide (alumina) and silicon carbide [26] are commonly used in high-temperature applications [27]. Examples include gas sensors [28, 29], pressure sensors [30] and microcombustors [31].

Co-fired ceramics are fabricated using techniques developed to make robust electronic components and circuit boards. These techniques utilize layers of tape-cast ceramic powder in their unfired form, also called green form, which are laminated on top of each other to create 3D-structures [32, 33]. Co-fired ceramics are divided into two groups: low-temperature co-fired ceramics (LTCC) and high-temperature co-fired ceramics (HTCC), where low temperature, in this case, refers to a firing temperatures of 900 to 1000 °C, as opposed to high-temperature, which relates to firing temperatures reaching up to 1800 °C. The difference stems from the materials used, where LTCC is a glass/ceramic composite where the glass fuses when fired, whereas HTCC is a pure ceramic which sinters. To create conductors, screen printing of metal pastes, typically silver for LTCC and platinum for HTCC, is used. Conductors can be printed on several layers, and connected through electrical vias to form electrical components and multi-layer circuit boards. These were originally used to mount silicon chips, and needed low dielectric constants, and a thermal expansion coefficient close to that of silicon.

Since then, LTCC in itself has been widely used for MEMS components like radio frequency (RF) circuits and microwave devices due to its favorable dielectric properties. HTCC is often used in packaging, but has also been used as a stand-alone substrate for pressure sensors, and yttria stabilized zirconia (YSZ) has been used for MEMS gas sensors, and solid oxide fuel cells (SOFC) [34] due to its high temperature stability, as well as its sensitivity to different oxygen partial pressures, which increases with elevated temperatures. Both LTCC and HTCC components have been proposed for use in aggressive environments [35, 36] as they survive higher operating temperatures than traditional silicon MEMS components [30,37]. However, for temperatures above 1000 °C, HTCC is the only viable option.

In **Paper III**, **IV**, and **V**, HTCC processing of 8 mol-% yttria stabilized zirconia (YSZ8) is used to fabricate thrusters and flow sensors. HTCC processing is relatively mature, in that it is an established technique, and most processing steps have been developed along with material in compatible formats, e.g., conductor pastes that adhere to HTCC substrates, sacrificial material, and substrates that can be laminated. The main challenge when using HTCC is the limited number of materials from which to chose. This is of course due to the high temperatures that the materials need to endure.

Aside from a high melting point, when selecting materials for high temperature applications, other parameters such as thermal conductivity [38] and thermal expansion need to be taken into consideration. Together, the latter parameters contribute to the material's their ability to withstand thermal gradients, i.e., thermal shock [39–41]. Thermal shock resistance is often characterized by water quenching of heated samples, after which the flexural strength is measured [42, 43]. The temperature after which the flexural strength is reduced to 70% of the unshocked value is called the thermal shock resistance temperature, ΔT_c.

Attempting MEMS manufacturing with new materials, it is also often necessary to develop new ways of fabrication. Working with a ceramic slurry, as in **Paper VI**, it is not possible to use plasma etch processes. Instead, a common tool for fabrication of ceramics is milling. Milling is relatively quick, but compared with other MEMS fabrications techniques, it has a very low precision and low resolution [44].

An alternative, when working with ceramics in green form is embossing or punching. In **Paper III**, silicon tools, fabricated with DRIE, are used to emboss and punch patterns in the ceramic tape, thereby achieving feature sizes comparable to those in silicon. This process allowed fabrication of a microthruster with dimensions similar to the silicon microthruster studied in **Paper I**.

In **Paper VI** a first step toward hafnium dioxide, or hafnia, MEMS is taken. Hafnia has a higher melting point than most other ceramics including alumina and stabilized zirconia [27, 45] which are the two most prevalent materials in HTCC. In **Paper VI**, hafnia powder is mixed with a dilutant and polymer components to form a slurry, which is then cast into polydimethylsiloxane (PDMS) molds. The molds were made by pouring PDMS over silicon masters, again allowing the use of silicon microfabrication techniques to create high-resolution patterns in a ceramic material. The patterns produced by casting had a high aspect ratio and also produced smooth side walls, and retained a good top-surface flatness. However, using the current recipe the material was more brittle in its green form than the zirconia tapes used in **Papers III**, **IV**, and **V**, which affected the yield in screen printing negatively. Despite using materials not designed to be compatible with hafnia, the printed results showed good adhesion to the substrate.

In addition, beams were fabricated in the same manner for measuring the Young's modulus of the material as well as its thermal shock resistance. Besides a higher melting point, Hafnia was found to have a higher thermal shock resistance than that of alumina and zirconia ceramics.

PDMS molds containing micrometer-scale test patterns were also fabricated to study the resolution, aspect ratio, and how well the shapes survived the replication process and sintering. In conclusion, **Paper VI** constitutes a good stepping stone for continued development in hafnia MEMS.

3. MEMS in space

Contrary, perhaps, to popular belief, the Wright brother's achievement was not the first human heavier-than-air flight. Rather, it was the first *powered* human heavier-than-air flight. This made possible truly independent transport, where humans were no longer simple passengers to winds, up-drafts, and hillsides, but could travel from point A to point B with purpose. The distinction is quite important both on earth and in space.

Because there is so much money to be saved by reducing the weight of spacecraft, often there is a willingness to sacrifice some performance or functionality in return for reduced mass. The prevalent form factor for small satellites at the moment is the so-called CubeSat [46]. A CubeSat is a $10\times10\times10$ cm cube weighing approximately 1 kg, Figure 3.1. By standardizing the dimensions, equipment does not need to be modified for individual launches, and parts of the satellite, such as solar panels and batteries, can be mass-produced. Figure 3.1 shows the PhoneSat "Graham" which uses a commercial off-the-shelf smartphone as its core. The smartphone already contains numerous cameras and sensors as well as radio and GPS receivers. A smartphone does not, however, include propulsion. This means that, while there are mature means to launch pico-satellites, so far, most are only radio beacons which verify their own presence in space before slowly losing speed to aerodynamic drag and burning up in the atmosphere on re-entry. A minority have any instruments or cameras on board, and fewer still contain propulsion systems.

However, even if the individual satellites are small and only carry limited useful payload, the inclusion of propulsion systems could enable the creation of clusters of formation flying spacecraft and the building of sensor networks from very small building blocks [47].

3.1 Micropropulsion systems

Conducting experiments in microgravity and very thin atmosphere may be enough to justify a space mission, and there is much that can be accomplished without directional control of a spacecraft, but most often, spacecraft need some type of propulsion system [48]. These are divided into electrical and chemical systems.

Figure 3.1. A model of the PhoneSat "Graham", a 1U CubeSat measuring 10×10×10 cm and weighing approximately 1 kg. Tea cup shown for scale. Courtesy NASA/JPL-Caltech.

A number of electrical micropropulsion systems have been demonstrated to this date. A review of the field has been presented by Wright and Ferrer [49] which summarizes the latest 15 years of development. Some examples include ion thrusters [50], which ionize a neutral gas propellant, pulsed plasma thrusters (PPT) [51], which ablate solid propellant into a plasma, and Hall thrusters [52,53], a type of plasma thruster which ionizes an inert neutral propellant in a Hall current loop. All these systems rely on accelerating ions to produce thrust. Some electric propulsion technologies have been developed specifically for micropropulsion systems, for example field emission electric propulsion (FEEP) [54,55], which uses liquid metal as propellant, and colloid thrusters [56, 57], which uses an ionic liquid as propellant in an electrospray nozzle – a working principle similar to FEEP, but expelling droplets instead of ions to produce thrust. The benefit of electric propulsion systems are their high fuel efficiency, in rockets and thrusters often defined as specific impulse, I_{sp}, but they are often difficult to miniaturize, as they can be complex or rely on complicated and bulky electronics or other large subsystems which may be beyond the size or mass budget of the craft [58, 59].

Chemical propulsion systems are generally simpler in operation, and therefore easier to miniaturize [49, 60]. Recent examples include monopropellant thrusters [61,62], in which the propellant decomposes in contact with a catalyst, bipropellant microthrusters [63], where a chemical reaction between two compounds occurs, and solid fuel microthrusters [64–67], where combustion of a solid propellant is initialized through ignition. Other chemical propulsion systems include vaporizing liquid [68–71] and heated cold-gas [72,73] microthrusters, the former boiling a liquid, typically water, and the latter relying on the heating of pressurized gas to produce thrust. These systems have in common that increasing the performance of the thruster often necessitate higher temperatures in the components. In the end, the choice of thruster comes down to the mission, and the required Δv.

Cold-gas thrusters typically have relatively low I_{sp}, but require very few supporting systems. Electric propulsion requires less propellant mass per unit thrust, but any additional power consumption requires larger batteries and/or larger solar panels for replenishing the batteries. The benefit of electric propulsion is that, given sunlight and solar panels, extending its capacity comes at a very low mass penalty, whereas cold gas thrusters rely on the energy of pressurized gas stored in a tank, where every planned maneuver adds mass and volume to the tank. This is further compounded by scaling, since if the length scale of a gas tank is reduced, the volume contained within is reduced by the cube of the length reduction. Due to their size and simplicity, however, they are still ideal for certain missions, such as the Philae lander in the Rosetta mission, which needed only small thrust during the landing on the comet 67p/Churyumov-Gerasimenko.

Chemical propulsion is governed by the equation

$$I_{sp} = \frac{1}{g}\sqrt{\frac{2kR_mT_0}{k-1}\left[1-\left(\frac{p_{out}}{p_{in}}\right)\right]^{\frac{k-1}{k}}}, \tag{3.1}$$

where g is the gravitational acceleration, k is the ratio of specific heat capacities, R_m the gas specific constant, T_0 the gas temperature, and p_{in} and p_{out} are the inlet and outlet pressures, respectively. Since g is a universal constant, k and R_m are dictated by the propellant, and p_{in} and p_{out} are design parameters of the nozzle it is evident that once the pro-

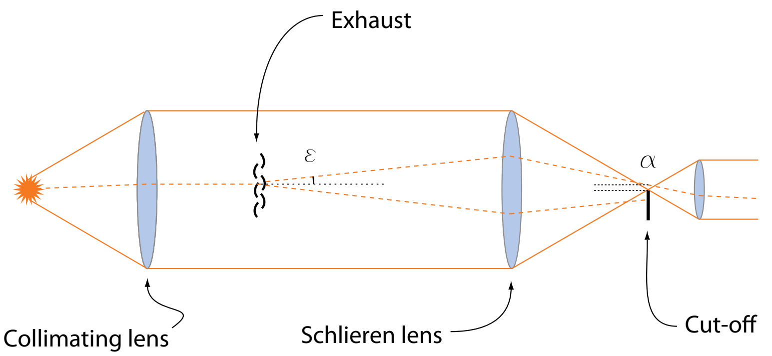

Figure 3.2. Schematic of the schlieren setup with the light-source shown at the far left, followed by the collimating lens, thruster exhaust, schlieren lens, cut-off, and focusing lens. A change in direction of the light passing through the exhaust, ε, will result in a shift of the beam at the cut-off, α.

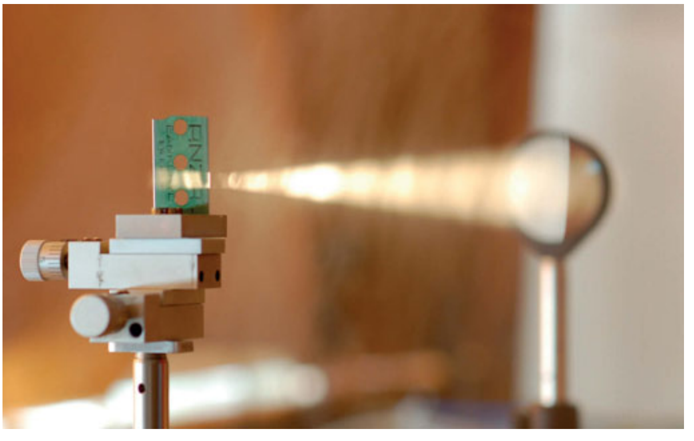

Figure 3.3. Cut-off and schlieren lens. The light beam is made visible using liquid nitrogen.

pellant is selected, the only way to improve the specific impulse is by increasing the temperature, T_0 of the gas. This has created a demand for microthrusters fabricated from high-melting point ceramics [69, 71], as in **Paper III**.

3.2 Schlieren imaging

Raising the temperature increases the specific impulse, but there are other ways to ensure the propellant is used efficiently. One is simply quality control. This is a challenge, as small leaks near the nozzle of microthrusters can be very difficult to detect. Another way is ensuring a straight thrust vector, again, due to the small scales and low thrust, this

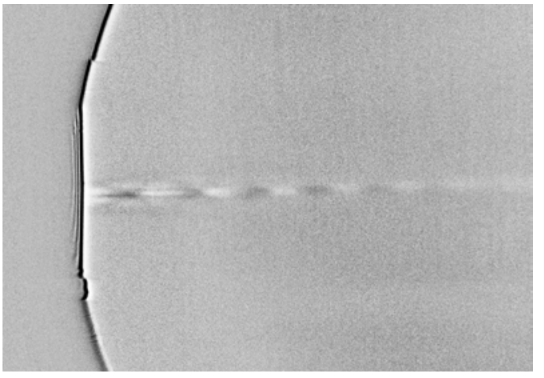

Figure 3.4. Schlieren image of exhaust from a working micronozzle in vacuum. Cut-off is perpendicular to exhaust, visualizing pressure differences within the flow. Field of view is 21×14 mm.

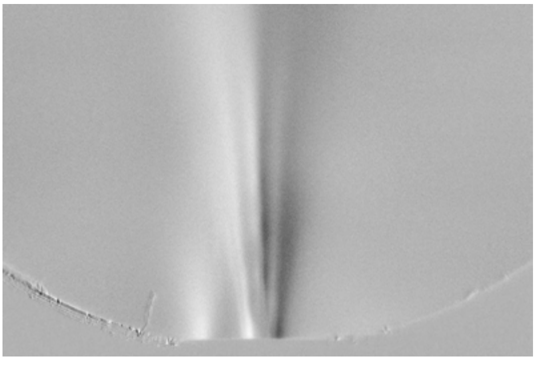

Figure 3.5. Schlieren image of a defective micronozzle in vacuum, exhibiting leakage problems. Leakage is visible as a small secondary exhaust next to the main exhaust. The cut-off is parallel with the flow, to visualize flow boundaries. Field of view is 21×14 mm.

is difficult to measure. Finally, precise flow control, measured as close to the nozzle as possible, ensures that the impulses are delivered with as much precision as possible.

Paper I demonstrates the use of schlieren imaging [74–76] to examine exhausts from cold-gas microthrusters. Schlieren imaging is a way to directly visualize changes or differences in refractive index within a material. The refractive index is a measure of the speed of light in a material, and the difference between refractive indexes will affect how much light refracts, or bends, when passing from one material to another. This can be compared to a person on roller skates, putting one skate on the grass by the side of the road. Because of the speed reduction on the grass, the skater will change direction toward the grass. When both skates are on the grass, the skater will have a completely new direction.

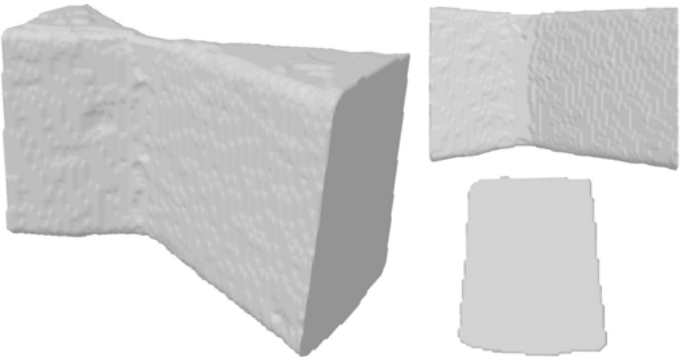

Figure 3.6. X-ray tomography of a DRIE-etched nozzle. Insets to the right are side and front views of the nozzle, to show RIE-lag (top) and underetching (bottom). The nozzle is approximately 30 μm wide and 380 μm deep at the narrowest part.

Figure 3.7. X-ray tomography of a close to circular cross-sectional nozzle. The nozzle is just under 50 μm wide at the narrowest point, and 230×290 μm at the exit, facing to the right.

To visualize this effect, a measurement set-up based on the principle shown in Figure 3.2 is required. In its simplest form, the set-up consists, from left to right, of a light source, a collimating lens, the schlieren lens, a cut-off, and finally a camera with a focusing lens. The collimating lens is placed with the light source in its focal point, to produce a beam of collimated, or parallel, light. Often, a system of lenses, which focuses the light source via an aperture or slit, is necessary to limit the extent of the source and improve the collimation. The sample or disturbance to be visualized is placed in the beam and followed by the schlieren lens. The schlieren lens focuses the beam of light onto a cut-off, Figure 3.3, while simultaneously focusing an image of the disturbance onto the camera. The cut-off is often simply a razor blade which can be moved into and

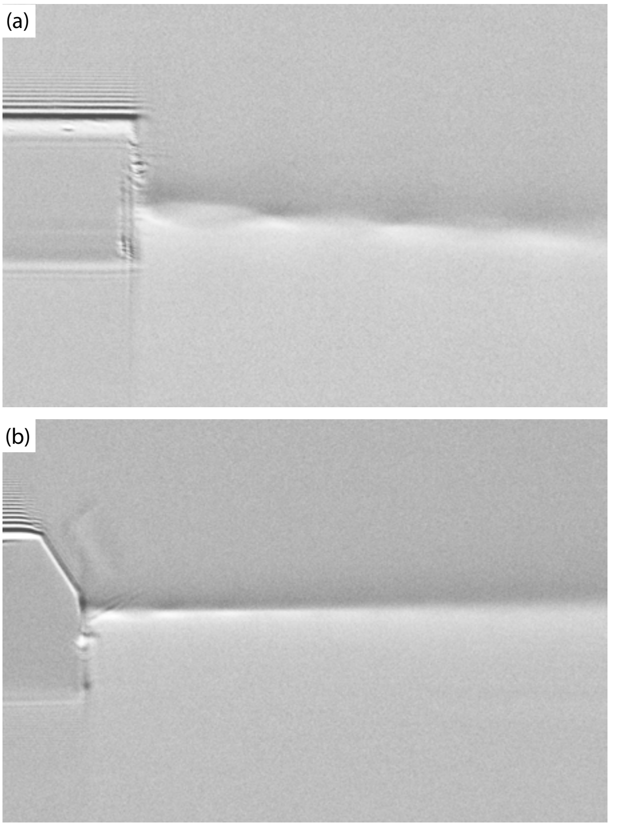

Figure 3.8. Schlieren images of exhausts from (a) a DRIE-etched micronozzle, and (b) a close to circular cross-section micronozzle. Exhausts are photographed perpendicular to the etch direction. Field of view is 3.6×2.4 mm.

out of the focal point of the schlieren lens, to block more or less of the undisturbed light. Any light that has refracted by the disturbance, i.e., changed direction (ε in Figure 3.2), will either pass freely by the cut-off (α) or be blocked by it completely. Due to the nature of the razor blade cut-off, only refraction in one dimension is visualized.

This method of visualizing gas flows was used to study the exhausts from micronozzles, Figure 3.4, and in the process, was shown to be a powerful tool to find leaks, Figure 3.5.

In **Paper II**, X-ray tomography and schlieren imaging were used to study the nozzle geometry and exhausts, respectively, from two different nozzles with either close to rectangular, Figure 3.6, or close to circular, Figure 3.7, cross-sections. It was found that RIE-lag and etch undercut caused an out-of-plane thrust vector in the DRIE etched nozzle. Schlieren images showed that the exhaust from the DRIE-etched nozzle deviated from the thruster plane by 2-3°, Figure 3.8. Besides using more propellant for the same impulse, this also introduces and unwanted impulse perpendicular to the desired thrust direction. This thrust needs to be counteracted, using even more propellant. The close to circular nozzle, for the first time demonstrated in **Paper II**, showed a symmetric and well aligned thrust vector.

3.3 Flow sensors

One important opportunity in MEMS fabrication is integration, where several components can share the same substrate. This contributes to weight reduction as well as moving the point of measurement close to the measurand. In **Papers III**, **IV**, and **V**, particularly flow sensors, and their integrability with microthrusters were investigated in detail.

To both monitor propellant consumption and to control precise maneuvers of a spacecraft, it is vital to be able to measure propellant flow to the thruster. The closer to the thruster that the flow can be measured, the better, since this will give more accurate real-time measurements of the impulse.

A straightforward flow sensor is the calorimetric anemometer. It relies on a heater, with two heat sensors on either side, patterned across a flow channel. When a flow is introduced in the channel, the thermal profile around the sensor shifts downstream, heating the downstream sensor and cooling the upstream sensor [77, 78]. A heater can simply be a conductor becoming warm when current is fed through it at sufficiently high power. The heat sensors, too, can be conductors, as most metals have a thermally dependent resistance, that is, the resistance increases with temperature. Hence, in its simplest embodiment the flow sensor consists of three parallel conductors across a channel.

A flow sensor of this type was integrated with the microthruster in **Paper III**. In this case, the sensor consisted of platinum conductors screen printed on zirconia HTCC. The flow sensor was seen to perform as expected, with signals in the mΩ/sccm-range, but when used while the nozzle heater was powered, thermal interference in the bulk prohibited reliable measurements.

To study the sensor principle in general, and the effect of thermal cross-talk in particular, a similar sensor was fabricated as a stand-alone component in **Paper IV**. In this sensor, additional conductors were patterned to make a total of five evenly spaced and identical conductors across the channel. They were each designed to allow four-point measurement of the resistance, in order to improve the accuracy by eliminating contact and lead resistances from the measurement. Using the center conductor as heater, the inner and outer conductor pairs were used as independent sensors. Furthermore, the outer-most conductors were used

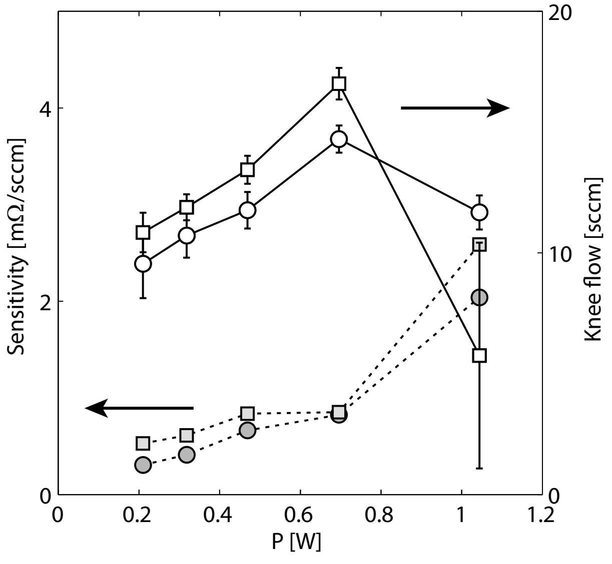

Figure 3.9. Sensitivity and measuring range, or knee flow, of the sensor, versus heater power. Sensitivity is indicated with dotted lines and left axis, knee flow with solid lines and right axis. Squares are measurements from a sensor with 160 μm separation between heater and sensors, circles from a sensor with 400 μm separation.

as auxiliary heaters, to study the influence of external heating on the performance of the inner sensor, as that observed in **Paper III**. It was found that an outside heat source shifted the response of the sensor in more or less the same way as a flow in that direction would.

It is expected that the conductors outside of the three central-most conductors could be used as auxiliary heaters in a flow sensor component to balance any such outside heat source, e.g., a thruster nozzle, hence, enabling close integration.

Moreover, when varying the power through the heater, it was seen that at a certain heater power, corresponding to a temperature of the sensor, the behavior of the sensor changed. Figure 3.9 shows the sensitivity along the left axis of the inner (squares) and outer (circles) flow sensors versus power. The measurement range of the sensor was defined as being from zero flow to a point where the sensitivity started decreasing, here called the knee flow. Above about 0.8 W heater power, the sensor response deviated from the common trend. Notably, the sensitivity increased dramatically, particularly for the sensor elements closer to the heater, and the knee flow decreased. The resistance between two adjacent conductors was measured while heating the component in a furnace. Above approximately 700 °C, the substrate resistance was low enough to significantly influence the sensor signal, Figure 3.10. This is due to ion conductivity in the substrate, which increases with temperature.

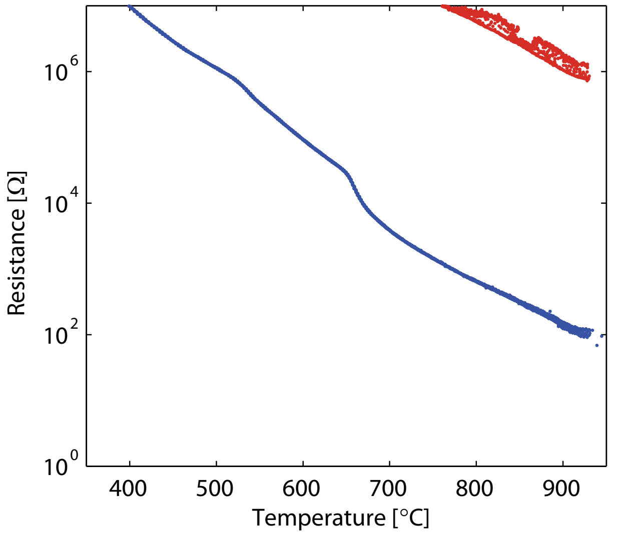

Figure 3.10. Resistance between adjacent conductors, 480 μm long and 80 μm wide on a zirconia substratate (blue) and hafnia substrate (red) versus temperature in a furnace.

Though this imposed a limitation in the traditional design, it offers an intriguing possibility to use the temperature dependence of ion conductivity as a sensing principle. This was investigated in **Paper V**, studying the same flow interval as in **Papers III** and **IV**, and produced a signal with nine orders of magnitude greater sensitivity. To our knowledge, this is the first ever implementation of this sensing principle. Because of the high sensitivity of the sensor, two adjacent conductors were used as heaters. This allowed for balancing of the sensor at zero flow, by adjustment of each heater individually. Not only does this make it possible for the sensor to function in elevated temperatures; it also enables the balancing of thermal gradients in the sensor, which may resolve the issue of thermal cross-talk seen previously. Furthermore, since it not only works in high temperatures but actually relies on these temperatures to operate, it will be possible to move the sensor into the stagnation chamber of the thruster and let the nozzle heater double as sensor heater to save power.

Another way to address the issue with ion conductivity is to choose a different material. Hafnia, studied in **Paper VI**, has a higher melting point than zirconia, and a resistance through the bulk four orders of magnitude lower than zirconia, when measure in the same way, Figure 3.10.

4. Conclusions and outlook

> "There is a single light of science, and to brighten it anywhere is to brighten it everywhere."
>
> — Isaac Asimov

The components and methods presented in this thesis have been developed keeping their use for space applications in mind. Each paper represents a small step toward smaller, more affordable, and more capable spacecraft enabling even small ideas to be realized – and to be realized without the need for backing by governments, international organizations or large corporations, but instead by groups of people who share a curiosity and a passion for space exploration.

Paper I demonstrates the use of schlieren imaging for simple and low cost characterization and quality screening of microthrusters. This test method is also used in **Paper II** to compare different fabrication methods. Here, the effects of RIE-lag, causing lower etch depth in the throat, contributed to an unexpected off-axis thrust vector from microthruster with a DRIE fabricated nozzle. Underetching may have further exacerbated this effect. Schlieren imaging was also used in **Paper III** to ensure no leaks were present and to verify a well-behaved exhaust at temperatures above 1000 °C.

Paper II focuses on the design of the nozzle, proposing a fabrication route which reduces viscous losses, and as a result, propellant consumption. An integrated flow sensor eliminates interfacing between the thruster and the sensor, which reduces both size, mass, and possible points of failure. Its proximity to the nozzle may also improve impulse control. Such flow sensors are studied more closely in **Paper IV**, where improvements are suggested and operating conditions identified. **Paper V** presents a new sensing method taking advantage of the ion conducting properties of the substrate as sensing principle, thereby allowing closer integration with the nozzle. It also enables the nozzle heater to double as sensor heater, which would reduce power consumption during operation. Finally, **Paper VI** demonstrates the first steps toward microfabrication in hafnium oxide – one of the highest melting point ceramics – a necessary transition to facilitate mono- or bipropellant thrusters in the microscale.

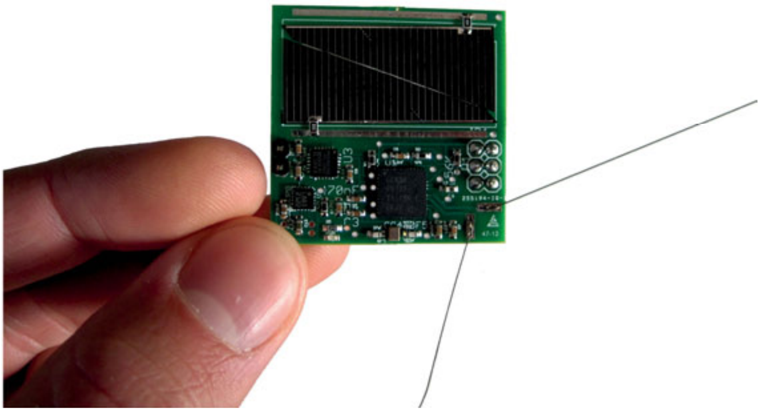

Figure 4.1. A *Sprite* femtosat, one of 104 daughter satellites to KickSat, weighing approximately 5 g each. Courtesy Zachary Manchester.

Through the use of space technology and research satellites, we have learned countless things about the history and composition of our planet and about life on earth. Our presence in space has enabled world-wide communication [79], global positioning systems [80], crop monitoring [81], pollution surveillance [82], weather forecasts [83, 84], and disaster management systems [85]. From memory foam mattresses [86] and the cordless vacuum [87], to medical monitoring systems developed for astronauts [88] and image processing techniques developed for the Hubble Space Telescope now in use for breast cancer detection [89], countless new technologies have seen use in people's everyday life on earth from the research that has gone into space exploration. Even companies not directly involved in the space program have developed products based on new requirements, such as the moon watch [90] and the space pen [91]. Many of these spin-off products and applications would not have come about, had it not been for the space programs of various countries. In many of these cases, the commercial use had not even been considered at the time the technology was conceived. The use of ceramics as substrate material in MEMS, demonstrated in **Papers III**, **IV**, **V**, and **VI** allows far higher operating temperatures than silicon and because of this may see use in any number on terrestrial applications from monitoring in processing industries to volcanic research.

Today, we stand before the next big revolution in space exploration. The so called "CubeSat" class of satellite has been developed as a standardized form factor for very small satellites, as a step toward reducing the the cost of satellite missions [92, 93]. Their smallest building block is a $10 \times 10 \times 10$ cm cube, with a mass limit of approximately 1 kg. A one unit, or 1U, CubeSat consists of one such cube. The standard can then be expanded to 2 or more concatenated cubes. Through this standardization, launchers do not need to be modified for individual payloads, and small satellites can be launched on short notice at low cost, and as piggyback payloads on larger launchers.

On April 18th, 2014, less than a year ago at the time of writing, *KickSat* [94] was launched from Cape Canaveral Air Force Station. KickSat itself was a rather unremarkable 3U CubeSat, but it was crowd funded. It was not the first crowd funded satellite; that first would be SkyCube [95] which was launched one and a half months prior. Nor was it the first time one satellite launched another. But what made KickSat so remarkable, was that it carried no less than 104 additional daughter satellites, or *sprites*, Figure 4.1, each weighing only approximately 5 grams, and each was privately owned, at a cost of $300. They all contained a solar panel, a microprocessor, and a transmitter sending out a unique identifier consisting of a few characters. This may not sound like much, but consider that this is more functionality than Sputnik 1, which arguably started the space race and weighed more than 10,000 times more and cost more than 100,000 times as much [96]. With this new dawn in space exploration, we can only imagine what technology will find new uses and where.

Imagine what these sprites might accomplish as fleets with propulsion systems – formation flying swarms forming optics with adaptable aperture and focal length, or autonomously linking together as building blocks to form a larger spacecraft. Space technology and microsystems technology have both come a long way in just a few decades. When it comes to the union of the two disciplines, we are just getting started!

5. Svensk sammanfattning

Människan har alltid haft en omättlig fascination för sin omgivning, såväl marken vi står på som himlavalvet. Länge troddes stjärnor och planeter vara spår av gudarna själva, kraftfulla verktyg för att förutspå framtiden, eller gudarnas sätt att kommunicera med människorna. Idag vet vi bättre, och i takt med att vår förståelse av fysik, biologi och kemi ökar, så ökar både förutsättningarna för, och viljan att, förstå ännu mer. Det kraftfullaste sättet att studera både himmel och jord är kanske från rymden. Men det är inte bara forskare som vill skjuta upp rymdsonder eller satelliter och det är inte bara för att sätta en flagga på månen eller leta efter vatten på Mars som det sker utveckling inom detta område.

Idag har rymdteknik en självklar plats i vår vardag. Det är svårt att hitta en mobiltelefon som inte innehåller en GPS-mottagare och liknande teknik finns i såväl kompaktkameror som klockor. Vi förutsätter tillförlitliga väderleksprognoser, högupplösta kartbilder och telefonkontakt med jordens alla hörn. Miljontals människor använder sig av denna teknik varje dag utan ett ögonblicks eftertanke och detta gör oss alla beroende av satelliter – några av de senaste decenniernas största vetenskapliga bedrifter. Det är förmodligen inte oförtjänt att raketforskning, i alla fall i engelskans dagliga tal, har kommit att representera något extremt komplex eller svårbegripligt. Ändå tas det helt för givet att vi ska kunna landa människor på Mars och att rymdturism ska vara ett semesteralternativ i en nära framtid. Allt detta tyder på att vi antingen ignorerar, glömmer, eller kanske mest troligt, helt enkelt inte inser den enorma insats som krävs för att utveckla och tillverka rymdfarkoster. Att skjuta upp en satellit är fortfarande i allra högsta grad en utmaning och är alltjämt förknippat med stor risk, höga kostnader och långa förberedelser.

Trots detta kommer man hela tiden på nya användningsområden för att fördjupa vår förståelse av jorden och solsystemet, för att utforska rymden, eller för att bättre förstå vårt osannolika ursprung. Oavsett tillämpning – kommersiell, militär, för forskning, eller rent av privat – är det angeläget att minska kostnaderna. För de två senare kategorierna är detta extra viktigt. Då uppskjutningskostnaden utgör en betydande del av den totala kostnaden för en rymdfarkost och denna kostnad är starkt förknippad med farkostens massa, kan den allmänna tillgängligheten till rymdteknik öka om farkosternas massa minskas. Men för att minska massan krävs användning av ny teknik. Häri ligger något av ett moment

22. På grund av de höga kostnaderna är toleransen för fel mycket låg. Detta leder till valet av beprövad teknik framför modernare, billigare, alternativ. Dock har teknik som kan minska massan hos rymdfarkoster med flera storleksordningar mognat markant de senaste åren och branschen börjar allt snabbare anamma den.

Mikroelektromekaniska system (MEMS) har sprungit ur elektronikindustrin som ett sätt att tillverka små elektromekaniska eller fluidala komponenter. MEMS-framställning använder ofta verktyg utvecklade för framtagning av halvledarelektronik, även om dessa används på något annorlunda sätt för att skapa de önskade strukturerna.

Mikro (μ) är ett prefix som anger 10^{-6} eller 0,000001 och 1 μm, den typiska storleksordningen för MEMS-komponenter, motsvarar ungefär en hundradel av tjockleken hos pappret i den här boken. Att krympa storleken på olika system kan dock vara mer eller mindre komplicerat. Vissa system måste ha en viss storlek på grund av fysikaliska begränsningar. Exempel på detta är antenner och optik, som båda samlar elektromagnetisk strålning. Antenner behöver ha en viss längd för att kunna registrera en fullständig våglängd hos strålningen och får sämre prestanda om den görs kortare. Optik samlar in ljus och storleken hos öppningen, eller aperturen, bestämmer signalstyrkan och därmed signal-tillbrus förhållandet i bilderna. På grund av fenomen som dessa, uppstår begränsningar av hur små vissa komponenter kan bli. Miniatyriseringar kan också leda till att kraven på komponenterna förändras. Om till exempel massan och därmed tröghetsmomentet hos en farkost minskar, så minskas även den kraft, eller impuls, som krävs för att orsaka en förändring i dess hastighet, riktning eller rotation.

Detta exempel relaterar till det som kallas skalning. När längdskalan minskar, minskar arean med kvadraten på längden. Samtidigt minskar volymen, och därmed massan, med kuben av längden. Beroende på tillämpning kan detta antingen vara till för- eller nackdel och, i vissa fall, kan minskningen av längden leda till att helt andra fysikaliska principer börjar dominera. Om till exempel ett större djur kliver ner i en sjö, dominerar gravitationen och det sjunker. För insekter är dock ytspänningen den dominerande kraften och de kan bekvämt röra sig på ytan. I makroskopisk fluidik domineras flöden av tröghetskrafter vilket orsakar virvlar och turbulens i exempelvis en vätska. I mikroskala domineras flödena av viskösa krafter och blir istället parallella, eller laminära, på grund av att en större del av flödet ligger nära en kanalvägg och därför påverkas av så kallade randeffekter.

När väl rymdfarkoster har skickats upp i rymden, är de i princip helt utelämnade åt sin omgivning. Styrkommandon kan skickas från marken, men förutom i extrema undantagsfall sker det varken underhåll eller service. Varje omdirigering av en kamera, solpanel eller antenn måste åstadkommas av rymdfarkosten själv. Detsamma gäller för all ompositionering av själva farkosten i sin bana (s. k. attitydkontroll), eller förändring av omloppsbanan, inklusive justeringar för att kompensera för hastighetsförluster på grund av luftmotstånd. För dessa manövrar krävs någon form av framdrivning. Oavsett tillämpning lyder sådana under Newtons rörelselagar – två kroppar som verkar på varandra utsätter varandra för lika stora men motriktade krafter. Bilhjul som roterar mot asfalt till exempel, utsätts för en kraft från asfalten som accelererar bilen framåt. I rymden uppstår kraften typiskt genom att massa kastas ut från ett munstycke vilket resulterar i en reaktiv kraft i motsatt riktning. Ett framdrivningssystem utgör allt som har med framdrivning att göra. I exemplet med bilen består framdrivningssystemet bland annat av bränsletank, motor, växellåda, drivlina och hjul.

Hos mikroframdrivning kan "mikro" syfta på två saker. Antingen refererar det till ett framdrivningssystem som levererar kraften av storleksordningen mikronewton (μN). Sådana system används för mycket precis positionering av större rymdfarkoster, till exempel rymdteleskopet Hubble. Mikro kan även avse miniatyriserade framdrivningssystem, ofta framställda med hjälp av MEMS-teknik, vilka inte med nödvändighet producerar just μN-stor dragkraft. Den förstnämnda kategorin har inte samma krav på maximal storlek eller massa, den sistnämnda kategorin kan utformas för att producera mer eller mindre dragkraft beroende på tillämpning. Dagens mikroframdrivning omfattar både elektriska och kemiska system.

Elektrisk framdrivning accelererar laddade partiklar i ett elektriskt fält för att skapa dragkraft. Detta kan ske bland annat genom blixturladdning (plasma) där joner accelereras i ett elektriskt fält, eller så kallad elektrospray, där droppar av laddad vätska accelereras med hjälp av en elektrisk potential. I allmänhet är elektrisk framdrivning väldigt effektiv, vilket är gynnsamt. Däremot är systemen ofta beroende av stor och komplicerad kringutrustning, till exempel spänningsaggregat som kan vara svåra att miniatyrisera.

Kemiska system använder kemiska reaktioner för att skapa dragkraft, till exempel genom förbränning eller sönderfall av ett drivmedel. Även kallgasraketer, som accelererar trycksatt gas genom ett munstycke, eller dysa, räknas till denna kategori. Kemiska framdrivningssystem, i motsats till elektriska, är i allmänhet mindre komplicerade, och lämpar sig därför väl för miniatyriserade farkoster. Exempel på kemisk framdrivning är fastbränsleraketer, som antänder ett bränsle i fast form, eller så kallade "bipropellant" raketer, där bränslet är uppdelat på två kemiska komponenter som startar en kemisk reaktion när de kommer i kontakt med varandra. Kallgasraketer skapar dragkraft genom att pressa ut en trycksatt gas genom en dysa. Utöver dysan kräver inte dessa system mycket mer än en bränsletank, en ventil och någon form av sensor för att övervaka bränsleförbrukningen, vilket gör dem attraktiva för de allra minsta rymdfarkosterna. Kallgasraketer lider dock typiskt av låg specifik impuls vilket är ett mått på effektivitet. Den specifika impulsen förbättras dock om gasen värms i dysan, och sådana system kallas något kryptiskt för varma kallgasdysor.

Syftet med denna avhandling är att presentera olika tillverknings- och avsyningsmetoder för varma kallgasmikroraketer. Detta för att kunna ta fram dysor och raketkomponenter som erbjuder bättre precision och bränsleeffektivitet än de idag existerande och som möjliggör en användning av andra kemiska framdrivningsprinciper i mikroskala. Vidare presenteras flödessensorer för nära integrering med dessa raketer.

I **Papper I** demonstreras användningen av schlierenavbildning som en enkel och billig metod metod för karakterisering och funktionstestning av mikroraketer. Denna testmetod användes också i **Papper II** för att jämföra två kiseldysor tillverkade med olika metoder. Här upptäcktes att asymmetrier orsakade av tillverkningsprocessen, som lägre etsdjup i dysans förträngning och ökad kanalbredd med ets-djup, bidragit till en oväntad fellinjering av dragkraftriktningen.

I **Papper II** studerades även raketmunstyckets utformning närmare, och ett tillverkningssätt för att åstadkomma dysor med förbättrad symmetri presenterades. Denna symmetri bidrar till minskade viskösa förluster, och därmed minskad drivmedelsförbrukning.

Schlierenavbildning användes också i **Papper III** i en studie av en keramisk raketkomponent för att bekräfta att dysan var tät och att utblåset var rakt. Här var dysan tillverkad av yttriumstabiliserad zirkoniumoxid – ett material som klarar arbetstemperaturer över 1000 °C.

Genom att integrera en flödessensor nära dysan kan komponentens storlek och massa minskas. Integrering reducerar även antalet kopplingar och gränssnitt, vilket minskar risken för läckage. Närheten till dysan kan också förbättra precisionen i mätningarna. Integrering av en flödessenor demonstrerades i **Papper III**, och dessa sensorer studerades närmare i **Papper IV**. I **Papper III** identifierades problem med termisk överhörning mellan dysa och sensor. Detta fenomen kartlades noggrannt och sätt att motverka det föreslogs. Dock identifierades ytterligare problem med elektrisk överhörning orsakade av jonledning i substratet vid temperaturer över 700 °C. Genom att istället betrakta jonledningen som en möjlighet, presenteras i **Papper V** en ny sensorprincip som utnyttjar temperaturberoendet hos de jonledande egenskaperna i det keramiska substratet, vilket möjliggör närmare integration med raketdysan. Detta gör att sensorn i sig kan användas för att värma dysan, vilket skulle kunna minska strömförbrukningen under drift. Slutligen, i **Papper VI** tas de första stegen mot tillverkning av mikrosystem i hafniumoxid. Hafniumoxid har en smältpunkt som är högre än de flesta andra keramer och lider inte av jonledning i samma utsträckning som dopad zirkoniumoxid. Den höga smältpunkten är en förutsättning för att tillåta en- eller tvåkomponentbränsle hos framtida kemiska mikroraketer.

De komponenter och metoder som presenteras i denna avhandling har utvecklats för användning i rymden. Varje papper utgör ett litet steg mot mindre, billigare och mer kapabla rymdfarkoster i syfte att göra rymdteknik tillgänglig för en bredare massa. De utgör därför ett steg mot att rymdprojekt kan förverkligas utan stöd av regeringar, internationella organisationer eller stora företag, utan istället av grupper av människor som delar en passion och en nyfikenhet för rymdforskning.

Idag står vi inför nästa stora revolution inom rymdforskningen. Som ett led i att minska uppskjutningkostnaderna har det tagits fram en standard för små satelliter, så kallade "CubeSats". Deras minsta byggsten utgörs av en 10×10×10 cm kub som har en viktbegränsning på cirka ett kilogram. En "one-unit", 1U, Cube-Sat består av en ensam sådan kub. Standarden kan sedan utvidgas till två eller flera hoplänkade kuber. Genom denna standardisering kan små satelliter skickas upp med relativt kort varsel och de kan även åka snålskjuts med andra större farkoster.

Den 18 april 2014, i skrivandets stund mindre än ett år sedan, sköts KickSat upp från Cape Canaveral. KickSat var i sig en ganska alldaglig CubeSat, även om den var gräsrotsfinansierad, det vill säga finansierad av ett stort antal privatpersoner som alla bidrog med små summor. Det som gjorde KickSat speciell var dock att den bar på 104 stycken dottersatelliter, eller "älvor", som var och en vägde cirka 5 g och var privatägda till en kostnad av drygt 2000 kronor. Varje älva innehöll en solpanel, en mikroprocessor, och en sändare som sände ut en unik identifieringssignal bestående av ett par tecken. Detta kanske inte låter så märkvärdigt men betänk då att detta ger dem mer funktionalitet än Sputnik 1, världens första satellit, även om Sputnik vägde mer än en tiotusen gånger mer och kostade mer än hudratusen gånger så mycket. Detta är skalning i sitt esse, och gör att vi står inför helt nya möjligheter inom rymdforskningen. Med de senaste decennierna i backspegeln kan vi bara gissa vad framtiden har att utvisa och hur rymdtekniken kommer att fortsätta påverka vår vardag.

Tänk vad dessa älvor skulle kunna åstadkomma om de förságs med framdrivningssystem – formationsflygande svärmar för optik med anpassningsbar bländare och brännvidd, eller med förmågan att länka ihop sig som byggstenar till en större rymdfarkost. Rymdteknik och mikrosystemteknik har båda nått stor mognad på bara ett par decennier och när det kommer till skärningspunkten mellan de två disciplinerna har vi bara sett början.

6. Acknowledgements

As a PhD student, inevitably, the colleagues with whom I started working are almost all long gone now that I'm finished, replaced by a whole new generation of PhD students. It was as a new PhD student that I got help from the more experienced, and usually not the other way around. My, and other PhD students', work is therefore based on a sort of pay-it-forward principle, where favors are passed on, rather than repaid. As I am laying down my pen after five years within these walls, it is with the sincere hope and genuine belief that I have done my part, repaying the favors to those who have come after me in the group and in the department, keeping the spirit alive. It is a natural progression of things, and I hope that those who have influenced me will know, whether or not they read these acknowledgments.

That having been said, I would like to take this opportunity to specifically acknowledge a number of people, who have had particular influence on my work.

I would like to thank Greger, for always being accessible and always having creative and inspiring ways to look at both problems and opportunities, both on project level and in the details. Thank you also for your effort in making ÅSTC a fun place to work. Thank you Henrik and Hugo for your support and welcoming to the group, and for the competent help in the lab. Thank you Lena, for joining the project at a stage when your experience was as crucial as your kindness and enthusiasm – your passion for the field is truly inspiring. Thank you also to Klas, for the work you put in to make this, and many other PhD projects, as well as the division as a whole, successful. I have enjoyed working closer with you during the final stages of my PhD.

I would like to thank the original ÅSTC; Martin, Johan, Jonas, Sara, Kristoffer – who started out as a supervisor but ended up a valued collegue, and Anders – who started out as a colleague but ended up a valued supervisor. You all made the choice to join and stay in the group very easy, and you have been instrumental in creating a fantastic working environment.

I would also like to thank the rest of the division, Stefan, Seung Hee, Minghzi, Tao, Athena, Peter, as well as the newcomers, Martin and Frida. It is a true pleasure seeing and working with such diverse talents, in such a seemingly narrow field as MEMS. My faith in the future of microsystems technology rests calmly on your shoulders.

Outside of the microsystems group, a few people deserve special recognition: I probably would not have considered working at the department, had it not been for Frida, Julia, Benny, Johanna, and Janna of the tribology group. You introduced me to a workplace that was incredibly friendly, with people as kind and helpful as yourselves, no doubt carefully selected by the seniors.

These same seniors continue their outstanding recruitments, and I would therefore like to thank the current tribo and MIM groups, for the awesome atmosphere we have at the fikas, lunches and parties. Sorry about the chairs.

Thank you Anja, Karin, Sara, and Per-Richard for keeping this workplace up and running, and thank you to human resources, particularly Eva, Ingrid, Maria and Maria, for all your help with all the various questions I've had throughout the years.

An emphatic thank you also to Jonatan, for the instant and ceasless help with my various computers and odd requests, and for the great discussions at fika.

Thank you MSL for maintaining the cleanroom and responding to all sorts of incidents all hours of the day and all days of the week. A particular thank you to Janne for helping out far beyond his responsibilities, and Victoria for expert assistance in the lab, as well as with the thesis. I am glad to have you as my friend.

The Knut and Alice Wallenberg foundation is acknowledged for laboratory funding. Vinnova and the Swedish National Space Board are gratefully acknowledged for funding many of my research projects.

Thank you to my family and friends for your understanding and patience, and for keeping me in touch with the real world.

Emilia, thank you for putting up with all the long days and late nights. Thank you for the tireless encouragement and selfless support that you have given, and keep giving. Thank you for laughing at my jokes, even when I am tired and they don't make sense. Thank you for your love. With you, this was possible.

Thank you also to Edvard, for reminding me what is important.

Finally, I want to thank everyone with whom I've shared casual conversation during coffee breaks, whose humor I've enjoyed during lunch breaks, whose gestures of everyday kindness I have appreciated, whose help I have received in the lab, in the library, or anywhere else – you are all part of making this happen. I wish I could name everyone, who, even by the smallest interaction have helped me achieve what is presented in this thesis,

but since I cannot, reader, look
not at the acknowledgements, but at this book.

References

[1] J K Ziemer and S M Merkowitz. Microthrust propulsion of the LISA mission, in *40th AIAA Joint Propulsion Conference.* Fort Lauderdale, Florida, July 12-14 2004.

[2] G Saccoccia, J Gonzalez del Amo, and D Estublier. Electric propulsion: A key technology for space missions in the new millenium. *ESA bulletin*, 2000.

[3] C A Mack. Fifty years of Moore's law. *Semiconductor Manufacturing, IEEE Transactions on*, 24(2):202–207, May 2011.

[4] G P Sutton and O Biblarz. *Rocket Propulsion Elements*. John Wiley & Sons, Inc., New York, 2001.

[5] J R Wertz and W J Larson, editors. *Space Mission Analysis and design*. Microcosm Press and Kluwer Academic Publishers, USA, 3rd edition, 2003.

[6] J C Whitehead. Single stage to orbit mass budgets derived from propellant density and specific impulse. *AIAA paper, July*, 1996.

[7] W J Pomerantz and S J Isakowitz. Virgin galactic. *New Space*, 1(4):167–170, 2013.

[8] G C Hudson. Quickreach responsive launch system. In *Paper No. RS4-2006-2003, presented at 4th Responsive Space Conference, Los Angeles, CA*, 2006.

[9] Airborne launch assist space access (ALASA). Website, accessed March 2015. http://www.darpa.mil/Our_Work/TTO/Programs/Airborne_Launch_Assist_Space_Access_(ALASA).aspx.

[10] S Cass. MEMS in space. *Spectrum, IEEE*, 38(7):56 –61, July 2001.

[11] T-A Grönland, P Rangsten, M Nese, and M Lang. Miniaturization of components and systems for space using MEMS-technology. *Acta Astronautica*, 61(1):228–233, 2007.

[12] H R Shea. MEMS for pico- to micro-satellites. In *Proc. SPIE*, volume 7208, page 72080M, 2009.

[13] N F de Rooij, S Gautsch, D Briand, C Marxer, G Mileti, W Noell, H R Shea, U Staufer, and B van der Schoot. MEMS for space. In *Solid-State Sensors, Actuators and Microsystems Conference, 2009. TRANSDUCERS 2009. International*, pages 17–24. IEEE, 2009.

[14] M J Madou. *Fundamentals of Microfabrication: The Science of Miniaturization*. CRC Press, Washington D.C., second edition, 2002.

[15] S Franssila. *Introduction to microfabrication*. Wiley, 2004.

[16] A A Ayón, R L Bayt, and K S Breuer. Deep Reactive Ion Etching: a promising technology for micro- and nanosatellites. *Smart Materials and Structures*, 10:1135–1144, 2001.

[17] M C Louwerse, H V Jansen, M N W Groenendijk, and M C Elwenspoek. Nozzle fabrication for micropropulsion of a microsatellite. *Journal of Micromechanics and Microengineering*, 19(4):045008, 2009.

[18] K Gantz, L Renaghan, and M Agah. Development of a comprehensive model for RIE-lag-based three-dimensional microchannel fabrication. *Journal of Micromechanics and Microengineering*, 18(2):025003, 2008.
[19] P Zellner, L Renaghan, Z Hasnain, and M Agah. A fabrication technology for three-dimensional micro total analysis systems. *Journal of Micromechanics and Microengineering*, 20(4):045013, 2010.
[20] H Jansen, M de Boer, R Wiegerink, N Tas, E Smulders, C Neagu, and M Elwenspoek. RIE lag in high aspect ratio trench etching of silicon. *Microelectronic Engineering*, 35(1):45–50, 1997.
[21] C Hedlund, H-O Blom, and S Berg. Microloading effect in Reactive Ion Etching. *Journal of Vacuum Science & Technology A*, 12(4):1962–1965, 1994.
[22] V Domnich, Y Aratyn, W M Kriven, and Y Gogotsi. Temperature dependence of silicon hardness: Experimental evidence of phase transformations. *Reviews on Advanced Materials Science*, 17:33–41, 2008.
[23] K F Jensen. Microreaction engineering – is small better? *Chemical Engineering Science*, 56(2):293–303, 2001.
[24] H A Spang III and H Brown. Control of jet engines. *Control Engineering Practice*, 7(9):1043–1059, 1999.
[25] G A Landis. Robotic exploration of the surface and atmosphere of Venus. *Acta Astronautica*, 59(7):570–579, 2006.
[26] R Maboudian, C Carraro, D G Senesky, and C S Roper. Advances in silicon carbide science and technology at the micro- and nanoscales. *Journal of Vacuum Science & Technology A*, 31(5):050805, 2013.
[27] C B Carter and M G Norton. *Ceramic materials: science and engineering*. Springer Science & Business Media, 2007.
[28] S Yu, Q Wu, M Tabib-Azar, and C-C Liu. Development of a silicon-based yttria-stabilized-zirconia (YSZ), amperometric oxygen sensor. *Sensors and Actuators B: Chemical*, 85(3):212–218, 2002.
[29] Y-I Bang, K-D Song, B-S Joo, J-S Huh, S-D Choi, and D-D Lee. Thin film micro carbon dioxide sensor using MEMS process. *Sensors and Actuators B: Chemical*, 102(1):20–26, 2004. Selected papers from Transducers 03.
[30] M A Fonseca, J M English, M von Arx, and M G Allen. Wireless micromachined ceramic pressure sensor for high-temperature applications. *Microelectromechanical Systems, Journal of*, 11(4):337–343, August 2002.
[31] Z Khaji, P Sturesson, K Hjort, L Klintberg, and G Thornell. Investigation of the storage and release of oxygen in a Cu-Pt element of a high-temperature microcombustor. In *Journal of Physics: Conference Series*, volume 557, page 012078. IOP Publishing, 2014.
[32] K A Peterson, K D Patel, C K Ho, S B Rohde, C D Nordquist, C A Walker, B D Wroblewski, and M Okandan. Novel microsystem applications with new techniques in low-temperature co-fired ceramics. *International Journal of Applied Ceramic Technology*, 2(5):345–363, 2005.
[33] Y Imanaka. *Multilayered low temperature cofired ceramics (LTCC) technology*. Springer-Verlag, Inc., New York, 2005.
[34] K Kendall and S C Singhal. *High Temperature Solid Oxide Fuel Cells: Fundamentals, Design and Applications*. Elsevier Oxford, UK, 2003.

[35] J Xiong, Y Li, Y Hong, B Zhang, T Cui, Q Tan, S Zheng, and T Liang. Wireless LTCC-based capacitive pressure sensor for harsh environment. *Sensors and Actuators A: Physical*, 197(0):30 – 37, 2013.

[36] P Sturesson, Z Khaji, S Knaust, J Sundqvist, L Klintberg, and G Thornell. Thermomechanical stability and integrability of an embedded ceramic antenna with an integrated sensor element for wireless reading in harsh environments. In *Journal of Physics: Conference Series*, volume 476, page 012055. IOP Publishing, 2013.

[37] Q Tan, H Kang, J Xiong, L Qin, W Zhang, C Li, L Ding, X Zhang, and M Yang. A wireless passive pressure microsensor fabricated in HTCC MEMS technology for harsh environments. *Sensors*, 13(8):9896–9908, 2013.

[38] K W Schlichting, N P Padture, and P G Klemens. Thermal conductivity of dense and porous yttria-stabilized zirconia. *Journal of materials science*, 36(12):3003–3010, 2001.

[39] T J Lu and N A Fleck. The thermal shock resistance of solids. *Acta Materialia*, 46(13):4755–4768, 1998.

[40] J W Zimmermann, G E Hilmas, and W G Fahrenholtz. Thermal shock resistance of ZrB_2 and ZrB_2–30% SiC. *Materials Chemistry and Physics*, 112(1):140–145, 2008.

[41] M Ishitsuka, T Sato, T Endo, and M Shimada. Thermal shock fracture behaviour of ZrO_2 based ceramics. *Journal of materials science*, 24(11):4057–4061, 1989.

[42] D P H Hasselman. Unified theory of thermal shock fracture initiation and crack propagation in brittle ceramics. *Journal of the American Ceramic Society*, 52(11):600–604, 1969.

[43] H Awaji and S M Choi. Thermal shock tests and thermal shock parameters for ceramics. *Journal of the Korean Ceramic Society*, 49(4):385–396, 2012.

[44] C R Friedrich and M J Vasile. Development of the micromilling process for high-aspect-ratio microstructures. *Microelectromechanical Systems, Journal of*, 5(1):33–38, Mar 1996.

[45] C E Curtis, L M Doney, and J R Johnson. Some properties of hafnium oxide, hafnium silicate, calcium hafnate, and hafnium carbide. *Journal of the American Ceramic Society*, 37(10):458–465, 1954.

[46] H Heidt, J Puig-Suari, A Moore, S Nakasuka, and R Twiggs. Cubesat: A new generation of picosatellite for education and industry low-cost space experimentation. 2000.

[47] D J Barnhart. Very small satellite design for space sensor networks. Technical report, DTIC Document, 2008.

[48] J Bejhed. *Fluid Microsystems for Micropropulsion Applications in Space*. PhD thesis, Uppsala University, 2006.

[49] W P Wright and P Ferrer. Electric micropropulsion systems. *Progress in Aerospace Sciences*, 2014.

[50] J S Sovey, V K Rawlin, and M J Patterson. Ion propulsion development projects in US: space electric rocket test I to deep space 1. *Journal of Propulsion and Power*, 17(3):517–526, 2001.

[51] P V Shaw. *Pulsed plasma thrusters for small satellites*. PhD thesis, University of Surrey, 2011.

[52] K Komurasaki and Y Arakawa. Performance calculation of hall thrusters. *Acta Astronautica*, 38(3):185 – 192, 1996.

[53] D M Goebel and I Katz. *Fundamentals of electric propulsion: ion and Hall thrusters*, volume 1. John Wiley & Sons, 2008.

[54] J Mitterauer. Field emission electric propulsion: Emission site distribution of slit emitters. *Plasma Science, IEEE Transactions on*, 15(5):593 –598, oct. 1987.

[55] C A Scharlemann, A Genovese, N Buldrini, R Schnitzer, M Tajmar, H Früholz, and R Killinger. Status of the indium FEEP micropropulsion subsystem development for LISA pathfinder. In *Proceedings of the International Electric Propulsion Conference (IEPC'07)*, 2007.

[56] J Xiong, Z Zhou, X Ye, X Wang, Y Feng, and Y Li. A colloid micro-thruster system. *Microelectronic Engineering*, 61–62:1031–1037, 2002.

[57] R Krpoun and H R Shea. Integrated out-of-plane nanoelectrospray thruster arrays for spacecraft propulsion. *Journal of Micromechanics and Microengineering*, 19(4):045019, 2009.

[58] M Capacci, G Matticari, M Materassi, and G Noci. Development and qualification of a neutralizer device for the FEEP micro propulsion on microscope and LISA pathfinder. In *Proceedings of the international electric propulsion conference, IEPC*, volume 154, Forence, Italy, 2007.

[59] L Ceruti and A Polli. An adaptable power control unit for ion thruster micro-propulsion subsystems. In *Proceedings of the thirty-second international electric propulsion conference, Electric Rocket Propulsion Society*, Wiesbaden, Germany, 2011.

[60] J Köhler, J Bejhed, H Kratz, U Lindberg, K Hjort, and L Stenmark. A hybrid cold gas microthruster system for spacecraft. *Sensors and Actuators*, 97–98:587–598, 2002.

[61] M-H Wu and R A Yetter. A novel electrolytic ignition monopropellant microthruster based on low temperature co-fired ceramic tape technology. *Lab on a Chip*, 9(7):910–916, 2009.

[62] J Huh and S Kwon. Design, fabrication and thrust measurement of a micro liquid monopropellant thruster. *Journal of Micromechanics and Microengineering*, 24(10):104001, 2014.

[63] M-H Wu and P-S Lin. Design, fabrication and characterization of a low-temperature co-fired ceramic gaseous bi-propellant microthruster. *Journal of Micromechanics and Microengineering*, 20(8):085026, 2010.

[64] D Teasdale, V Milanovic, P Chang, and K S J Pister. Microrockets for smart dust. *Smart Materials and Structures*, 10(6):1145, 2001.

[65] C Rossi, D Briand, M Dumonteuil, T Camps, P Q Pham, and N F de Rooij. Matrix of 10$\times$10 addressed solid propellant microthrusters: Review of the technologies. *Sensors and Actuators A: Physical*, 126(1):241–252, 2006.

[66] D Seo, J Lee, and S Kwon. The development of the micro-solid propellant thruster array with improved repeatability. *Journal of Micromechanics and Microengineering*, 22(9):094004, 2012.

[67] J Lee and T Kim. MEMS solid propellant thruster array with micro membrane igniter. *Sensors and Actuators A: Physical*, 190:52–60, 2013.

[68] P Kundu, T K Bhattacharyya, and S Das. Design, fabrication and performance evaluation of a vaporizing liquid microthruster. *Journal of Micromechanics and Microengineering*, 22(2):025016, 2012.
[69] K H Cheah, P S Khiew, and J K Chin. Fabrication of a zirconia MEMS-based microthruster by gel casting on PDMS soft molds. *Journal of Micromechanics and Microengineering*, 22:095013, 2012.
[70] K Karthikeyan, S K Chou, L E Khoong, Y M Tan, C W Lu, and W M Yang. Low temperature co-fired ceramic vaporizing liquid microthruster for microspacecraft applications. *Applied Energy*, 97:577–583, 2012.
[71] K H Cheah and K-S Low. Fabrication and performance evaluation of a high temperature co-fired ceramic vaporizing liquid microthruster. *Journal of Micromechanics and Microengineering*, 25(1):015013, 2015.
[72] J Cardin and J Acosta. Design and test of an economical cold gas propulsion system. In *Proceedings of 14th Annual AIAA/USU Conference on Small Satellites*, pages 1–13, Logan, UT, USA, August 21–24 2000.
[73] V Lekholm, A Persson, K Palmer, F Ericson, and G Thornell. High-temperature zirconia microthruster with an integrated flow sensor. *Journal of Micromechanics and Microengineering*, 23(5), 2013.
[74] G S Settles. *Schlieren and Shadowgraph Techniques*. Springer–Verlag, Berlin, 1st edition, 2001.
[75] S D Scroggs and G S Settles. An experimental study of microjets. *Experiments in Fluids*, 21:401–409, 1996.
[76] C Huang, J W Gregory, and J P Sullivan. A modified schlieren technique for micro flow visualization. *Measurement Science and Technology*, 18:N32–N34, 2007.
[77] M Elwenspoek. Thermal flow micro sensors. In *Semiconductor Conference, 1999. CAS '99 Proceedings*, volume 2, pages 423–435, Sinaia, Romania, Oct 1999.
[78] K Palmer, H Kratz, H Nguyen, and G Thornell. A highly integratable silicon thermal gas flow sensor. *Journal of Micromechanics and Microengineering*, 22:065015, 2012.
[79] M Toyoshima. Trends in satellite communications and the role of optical free-space communications [invited]. *Journal of Optical Networking*, 4(6):300–311, 2005.
[80] R M Alkan, H Karaman, and M Sahin. GPS, GALILEO and GLONASS satellite navigation systems & GPS modernization. In *Recent Advances in Space Technologies, 2005. RAST 2005. Proceedings of 2nd International Conference on*, pages 390–394. IEEE, 2005.
[81] K P Gallo and T K Flesch. Large-area crop monitoring with the NOAA AVHRR: estimating the silking stage of corn development. *Remote Sensing of Environment*, 27(1):73–80, 1989.
[82] Y Liu, X Wang, M Guo, and H Tani. Mapping the FTS SWIR L2 product of XCO_2 and XCH_4 data from the GOSAT by the Kriging method–a case study in East Asia. *International journal of remote sensing*, 33(10):3004–3025, 2012.
[83] P K Rao, S J Holmes, R K Anderson, J S Winston, and P E Lehr. Weather satellites: Systems, data, and environmental applications. 1990.

[84] E W Holroyd III. Lake-effect cloud bands as seen from weather satellites. *Journal of the Atmospheric Sciences*, 28(7):1165–1170, 1971.

[85] S Voigt, T Kemper, T Riedlinger, R Kiefl, K Scholte, and H Mehl. Satellite image analysis for disaster and crisis-management support. *Geoscience and Remote Sensing, IEEE Transactions on*, 45(6):1520–1528, 2007.

[86] R S Schmidt. NASA pressure-relieving foam technology is keeping the leading innerspring mattress firms awake at night. *Technovation*, 29(3):181–191, 2009.

[87] C Conger. 10 NASA inventions you might use every day. *Discovery Channel. Np, nd Web*, 28, 2013.

[88] N P Ruzic. Spinoff 1976: A bicentennial report. *NASA Technical report*, 1976.

[89] G B Lubkin. Astronomical image processing may improve breast cancer diagnostics. *Phys. Today*, 48(6):21, 1995.

[90] N Smith. Timing for success. *Engineering & Technology*, 4(9):76–77, 2009.

[91] C Curtin. NASA spent millions on a pen able to write in space. *Scientific American*, 297(2):104–104, 2007.

[92] J Puig-Suari, C Turner, and W Ahlgren. Development of the standard CubeSat deployer and a CubeSat class picosatellite. In *Aerospace Conference, 2001, IEEE Proceedings*, volume 1, pages 1–347. IEEE, 2001.

[93] A Toorian, K Diaz, and S Lee. The CubeSat approach to space access. In *Aerospace Conference, 2008 IEEE*, pages 1–14. IEEE, 2008.

[94] Z Manchester, M Peck, and A Filo. Kicksat: A crowd-funded mission to demonstrate the world's smallest spacecraft. In *Proceedings of the AIAA/USU Conference on Small Satellites*, 2013.

[95] SkyCube: The first satellite launched by you. Website, accessed March 2015. http://www.southernstars.com/skycube/index.html.

[96] A P Cracknell and C A Varotsos. Editorial and cover: Fifty years after the first artificial satellite: from Sputnik 1 to ENVISAT. *International Journal of Remote Sensing*, 28:2071–2072, 2007.

Acta Universitatis Upsaliensis

Digital Comprehensive Summaries of Uppsala Dissertations from the Faculty of Science and Technology 1233

Editor: The Dean of the Faculty of Science and Technology

A doctoral dissertation from the Faculty of Science and Technology, Uppsala University, is usually a summary of a number of papers. A few copies of the complete dissertation are kept at major Swedish research libraries, while the summary alone is distributed internationally through the series Digital Comprehensive Summaries of Uppsala Dissertations from the Faculty of Science and Technology. (Prior to January, 2005, the series was published under the title "Comprehensive Summaries of Uppsala Dissertations from the Faculty of Science and Technology".)

Distribution: publications.uu.se
urn:nbn:se:uu:diva-246057

ACTA
UNIVERSITATIS
UPSALIENSIS
UPPSALA
2015